

UTILIZATION OF POPULATION BALANCES IN SIMULATION OF LIQUID-LIQUID SYSTEMS IN MIXED TANKS

Ville Alopaeus^{*1}, Kari I. Keskinen^{1,2}, Jukka Koskinen¹

¹Neste Engineering Oy, P.O.B. 310, FIN-06101, Porvoo, Finland

²Helsinki University of Technology, Laboratory for Chemical Engineering and Plant Design,
P.O.B. 6100, FIN-02015 HUT, Espoo, Finland

^{*}Corresponding author, Tel. +358 10 45 27493, Fax +358 10 45 27221

E-mail: Ville.Alopaeus@fortum.com

Keywords: population balances, mixing, liquid-liquid dispersion, inhomogeneity

Prepared for presentation of the 2000 Annual Meeting, Los Angeles, CA, Nov. 12-17

Copyright © Ville Alopaeus, Neste Engineering Oy, Finland

AICHE shall not be responsible for statements or opinions contained in papers or printed in its
publications

Abstract

A simulation model has been developed to model drop populations in a stirred tank. A multiblock stirred tank model has been used with the drop population balance equations developed in the literature. The drop breakage and coalescence functions used in the population balance model take into account the local turbulent energy dissipation values. The drop breakage and coalescence function parameters are fitted against drop size measurements from dense liquid-liquid dispersions, which were assumed fully turbulent. Since the local turbulence and flow values of a stirred tank are used in the present model, the fundamental breakage and coalescence phenomena can be taken into closer examination. Furthermore, the present model is capable in predicting inhomogeneities occurring in a stirred tank. It is also considered as an improved tool for process scale-up, compared to the simple vessel-averaged population balance approach, or use of correlations of dimensionless numbers only. The present model can use two sources of data for fitting parameters in the drop rate functions. One is to use transient data of the measured drop size distribution as the impeller speed is changed. The other is to use time-averaged data measured at different locations of the stirred tank. Different flow regions can be chosen from direct measurements or from the CFD simulations in a straightforward manner. CFD flow simulation results can be used when no experimentally obtained flow conditions are available. This is especially useful for non-standard vessels, such as reactors containing cooling coils.

Introduction

Many chemical processes take place in stirred tank reactors where two immiscible liquid phases take part in a chemical reaction. In these processes the drop size distribution, and the heat and mass transfer resistance, often affect the product quality.

In two-phase reactors, the mass transfer between phases can be determined from the expressions for mass transfer fluxes and the mass transfer area. The determination of drop size distribution and thus the mass transfer area for liquid-liquid dispersions in a stirred tank is the main objective in this work. The drop size distribution may also vary considerably in different regions of the stirred tank, and this variation is taken into account in our simulation model.

The classical method for determining mass transfer area is based on the correlations for Sauter mean diameter for droplets, a_{32} . These correlations are usually derived for a stationary state, but additional provision is sometimes made to take transients into account. These correlations are averages for the whole vessel only. They do not give any information about the drop size distribution or possible inhomogeneities in the stirred tank. In this work, a population balance approach is applied in more complicated and general cases. This approach is applicable in case the drop rate functions are known or can be estimated.

The underlying idea in this work is that detailed stirred tank flow data is applied in the model formulation. This flow data can be obtained from a computational fluid dynamics (CFD) model or from flow measurements. When modeling population balances in turbulent

dispersions, the most important fluid flow properties are the local turbulent energy dissipation levels and the local velocities.

The drop size distribution is generated by different phenomena, which can be divided into different categories. These are the following. 1. Feed or discharge of droplets in a particular region of the vessel under consideration. 2. Relative velocities between the continuous phase and the dispersed droplets affect drop size distributions in different parts of the vessel. 3. Growth and nucleation of droplets. Droplet growth (or shrinkage) follows from mass transfer into the droplet or out from the droplet, or from those reactions that do not conserve volume. Nucleation follows when the system becomes thermodynamically unstable. 4. Breakage and coalescence of droplets. These processes are affected by the local mechanical conditions in the dispersion, i.e. turbulent energy dissipation and shear forces. Besides this, by physical properties, i.e. viscosity and density of the phases, interfacial tension, and other interfacial phenomena, such as the surface charge of the droplets.

Population Balance Model

For the chemically equilibrated liquid-liquid dispersion (no growth or shrinkage of droplets due to mass transfer or reaction), the discretized population balance equation for a unit volume can be written as

$$\begin{aligned} \frac{dY_i}{dt} = & Y_{i,in} + \sum_{j=i+1}^{nc} v(a_j) \beta(a_i, a_j) g(a_j) Y_j \Delta a + \sum_{j=1}^{\#(V_i/2)} F((a_i^3 - a_j^3)^{1/3}, a_j) Y_i Y_j \\ & - Y_{i,out} - g(a_i) Y_i - Y_i \sum_{j=1}^{\#(V_{nc} - V_i)} F(a_i, a_j) Y_j \end{aligned} \quad (1)$$

In order to work with the population balance equations, the drop rate functions describing breakage and coalescence must be defined as well as the daughter drop size distribution resulting from a breakage. These functions are presented in the literature with several sets of parameters. In most cases these functions are either developed for dilute systems (low volume fraction of the dispersed phase), or at least the measurements and corresponding parameter fitting has been carried out with dilute systems. Besides that, often the vessel inhomogeneities in drop size distributions have been neglected.

Care must be taken in applying the drop rate models. Different assumptions regarding microscale phenomena in the dispersion leads to different drop breakage and coalescence functions. When modeling drop breakage and coalescence, a proper set of physical assumptions must be chosen in order to retain any reasonable extrapolating possibility for systems with different physical properties and different turbulence conditions.

Stirred Tank Model

The breakage and coalescence phenomena are affected primarily by local turbulence dissipation. Turbulence is not homogenous in a stirred tank, so that near the impeller turbulence is several orders of magnitude greater than near the wall, or at the surface of the dispersion or at the bottom of the tank. The result is that breakage of the droplets occurs almost exclusively near the impeller. On the other hand, the impeller pumps dispersion all over the tank. Inhomogeneities in the tank will result if circulation in the tank is not sufficiently faster than the breakage and coalescence phenomena. Hence, local turbulent dissipation values with flow rates between different regions of the stirred tank should be considered when the population balances are calculated.

In CFD simulations the stirred tank is usually divided into tens of thousands control volumes, and in some cases, even up to a million. A complete CFD model with population balances calculated in each cell is thus considered too complicated, especially when fitting parameters to breakage and coalescence functions. Thus we average the results of these complicated models and use a simplified "freezed" flow model that includes only a few control volumes. It has also been assumed that a simplified model can reveal all the underlying phenomena regarding non-idealities in a stirred tank. Simplifying the flow fields can be made in a straightforward manner by averaging from the full scale CFD calculations. Also direct measurements can be utilized whenever they are available.

We divide the stirred tank into 11 subregions as shown in Figure 1, where one half of the tank is shown. Symmetry around the impeller axis is assumed.

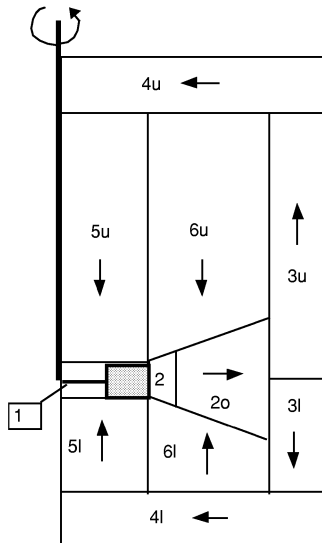


Figure 1. Subregions chosen for simulation in a stirred tank

The local turbulence dissipations in the different subregions, and flows between the subregions were obtained from the work of Bourne and Yu (1994). Here each subregion is assumed to be completely mixed and homogenous, so that volume averaging must be done in the following way for each region.

Average turbulent energy dissipation in the whole vessel is obtained from

$$\epsilon_{ave} = N_p D_i^5 N^3 / V. \quad (2)$$

It is assumed that all energy input to the vessel is dissipated by turbulent mechanisms.

The volume averaged relative turbulent dissipation is defined as

$$\phi = \epsilon / \epsilon_{ave}. \quad (3)$$

Relative turbulent dissipations and corresponding subregion volumes are given in Table 1.

Scaling is made here so that

$$\Sigma V_i = 1 \quad (4)$$

and

$$\Sigma V_i \phi_i = 1. \quad (5)$$

Table 1. Relative turbulent dissipations and volumes of different regions

Subregion	V_i	ϕ_i
1	0.0073	34
2i	0.0093	12
2o	0.0755	4.6
3u	0.2052	0.56
3l	0.0846	0.56
4u	0.0950	0.073
4l	0.1000	0.073
5u	0.0584	1.1
5l	0.0219	1.1
6u	0.2603	0.092
6l	0.0825	0.092

Internal flow patterns are needed for droplet convection between the subregions.

Dimensionless flow values (pumping numbers between the subregions) are here defined as

$$Q^*_{i,j} = Q / (N \cdot D_i^3). \quad (6)$$

These values are given in Table 2.

These values are adapted from the velocities presented by Bourne and Yu (1994), by taking their equation for radial flow rate in discharge

$$N_Q = Q^*_{1,2i} = Q / (N \cdot D_i^3) = 2.33 \cdot (r / D_i) - 0.379 \quad (7)$$

as a basis as the flow values are made consistent. These turbulent dissipation and flow values are quite comparable to our own CFD calculations.

Table 2. Dimensionless flow values (Q^*) between the subregions

from\to	1	2i	2o	3u	3l	4u	4l	5u	5l	6u	6l
1		0.7860									
2i			1.1006								
2o				1.3641	1.0492						
3u						1.3641					
3l							1.0492				
4u								0.4443		0.9198	
4l									0.3417		0.7075
5u	0.4443										
5l	0.3417										
6u		0.1778	0.7420								
6l		0.1368	0.5707								

Now the convection terms in the discretized population balance equation (1) can be calculated as

$$Y_{i,j,in} = \sum_{k=1}^{nb} \frac{Q_{kj} Y_{i,k}}{V_j} \quad \text{and} \quad Y_{i,j,out} = \sum_{k=1}^{nb} \frac{Q_{jk} Y_{i,j}}{V_j}, \quad (8)$$

where double indexed $Y_{i,j}$ is the number concentration of drop size i in block j , and the third index $_{in}$ or $_{out}$ again stands for convection speed in or out. Additional terms for convection into the vessel and out from the vessel must be added for a continuous flow operation.

Experimental

In order to verify the usefulness of the present model, some experiments with immiscible liquids were carried out, and the results were used to fit parameters of the drop breakage and coalescence rate functions. The laboratory vessel was a 50-liter standard stirred tank with four baffles. The stirrer was a six-bladed Rushton turbine, with which the speed can be set without step changes. The experimental system was an Exxsol in water-dispersion, and the volume fraction of the dispersed Exxsol was 0.4 in all experiments. This volume fraction is so high that the dispersion can be considered quite dense.

Exxsol is a commercial organic solvent, with the following measured physical properties at room temperature: density 800 kg/m^3 , viscosity 1.0 cP, and surface tension (against air) 24.4 mN/m. Interfacial tension between the organic solvent and water was obtained by subtracting the surface tension of Exxsol from the surface tension of water. The interfacial tension was 43.6 mN/m.

Drop size distributions were measured using a Lasentec® FBRM (Focused Beam Reflectance Measurement) device. It is based on a rapidly rotating laser beam. The measured property of the dispersion is the chord length distribution. This means that the laser beam randomly measures chord lengths of passing drops, and thus a distribution of chord lengths is obtained even for droplets of uniform size. The measured distribution must then be converted into a drop size distribution by assuming spherical droplets. This procedure is described by Tadayyon and Rohani (1998). The drop size range is divided into 38 channels, and the number of drops belonging to each of these channels is measured. Typically, several hundreds or thousands of drops are measured per second.

The present method seems to be one of the very few applicable to measure local drop size distributions in dense systems. It appears that the FBRM method still needs further validation and comparisons with other methods, but since there is a lack of other reliable drop size measurement methods, especially for dense and rapidly coalescing systems, the FBRM was the only method available to produce reasonable data for the parameter fitting.

It is proposed that the drop size distributions measured with the laser beam reflectance method may have some dependency on optical system-dependent properties. For a crude oil in water, the measured chord length distributions should be quite close to the correct ones, making the conversion to drop size distributions possible. Since Exxol is a crude oil distillate, we had confidence in the measured data (Haley, 1999).

In order to obtain statistically good results, ten sequential measurements were carried out at each of the three locations in the vessel. In the measurements, the stirring speed was first allowed to remain at a low value for some time to achieve the steady state distribution. After the steady state was reached, a step change was made, and the speed was doubled. After the steady state was reached for the higher speed, stirring was turned back to the lower speed. The time to ensure that steady state was reached was several times longer than the observed transient time after the step changes. Transients as well as steady states were measured at the three locations separately. The locations of the measurement points are shown in Figure 2.

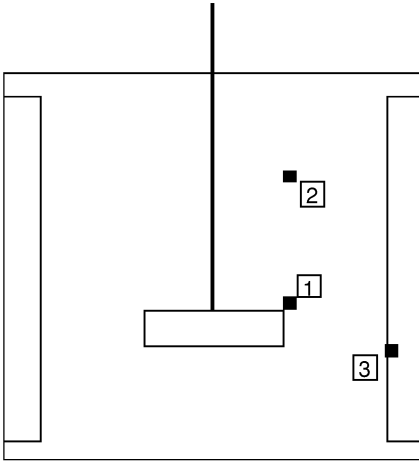


Figure 2. Locations of the measurement points in a stirred tank equipped with a six-blade Rushton turbine and four baffles

The stirring speeds were chosen according to two criteria. Firstly, complete suspension had to be obtained. This was observed from the surface of the dispersion. If large plates of the dispersed phase were floating on the surface, the impeller speed was too slow. On the other hand, if the speed was too high, air bubbles were intruded into the dispersion, severely disturbing the measurements. These two criteria indicated the operating window. For the test system, the range of reasonable stirring speeds was between 6.3 1/s and 12.57 1/s. These correspond to impeller Reynolds numbers of one to two hundred thousand, so that the system is well within the turbulent region.

These ten measured chord length distributions were then averaged. Some data was rejected due to “lumps” in the upper tail of the distribution. These appeared mainly at the higher impeller speed, lasting only one or two measurement time intervals. It was considered that

these measured values did not describe real drops, or the device was measuring some colliding drop clusters as one drop. Consequently, these measurements were omitted from the averaging process. After this averaging, the conversion to the drop size distributions was made for the parameter fitting procedure.

Parameter Fitting

At the first phase, the drop rate parameters were fitted using a one block system; i.e. the whole vessel was averaged by taking simply an arithmetic average of the measurements at the three locations. After that, the multiblock model was used, so that the measured distributions at different locations of the vessel were compared to the corresponding block values of the simulation model. The Nelder and Mead non-linear Simplex algorithm, followed by the Davidon and the Levenberg-Marquardt algorithms, were used in the fitting procedure. The residual for the fit was calculated from the error in the Sauter mean drop diameter and from the error in the shape of the volumetric population density, emphasis being on the Sauter mean diameter. The error in the shape of the population distribution was calculated by comparing measured and fitted population densities in four representative locations of the population distribution.

Various breakage and coalescence function forms found in the literature were tested. Most of them were not able to represent the data even qualitatively, and even many of those that were promising, appeared to have bad extrapolating characteristics. With any specified set of parameters, most of the functions showed unrealistic population distributions when physical properties or mixing conditions were varied. The following set of drop rate functions was

found to represent the data well, and showed reasonable characteristics in describing the population distributions generally.

For the **breakage frequency**, the following function was found to give good results:

$$g(a_i) = C_1 \epsilon^{1/3} \operatorname{erfc} \left(\sqrt{C_2 \frac{\sigma}{\rho_c \epsilon^{2/3} a_i^{5/3}} + C_3 \frac{\mu_D}{\sqrt{\rho_c \rho_D} \epsilon^{1/3} a_i^{4/3}}} \right). \quad (9)$$

This is based on drop breakage frequency function proposed by Narsimhan, Gupta & Ramkrishna (1979). The original form was extended by including viscous forces in the energy balance for drop breakage. Furthermore, all the parameters C_1 , C_2 , and C_3 were left as adjustable, and a dependency on energy dissipation to 1/3 power was assumed.

For the **drop coalescence**, the following functions are used. The drop collision term of Coalaloglou and Tavlarides (1977) is used. It stands as

$$h(a_i, a_j) = C_4 \frac{\epsilon^{1/3}}{1 + \phi} (a_i + a_j)^2 (a_i^{2/3} + a_j^{2/3})^{1/2}. \quad (10)$$

A simplified form of the coalescence efficiency function of Tsouris & Tavlarides (1994) is used (Alopaeus et al., 1999):

$$\lambda(a_i, a_j) = \left(\frac{0.26144\mu_D}{\mu_C} + 1 \right)^{P1}$$

$$P1 = \left(- \frac{C_5\mu_C}{\rho_C N_p^{1/3} \epsilon^{1/3} (a_i + a_j)^{2/3} D_i^{2/3}} \right). \quad (11)$$

The product of these two is then the **coalescence rate function** $F(a_i, a_j)$.

Yet the **daughter drop size function** needs to be specified. It gives the distribution of the formed drops when a breakage occurs. The following was found to give good results. (Bapat et al., 1983)

$$\beta(a_i, a_j) = \frac{90a_i^2}{a_j^3} \left(\frac{a_i^3}{a_j^3} \right)^2 \left(1 - \frac{a_i^3}{a_j^3} \right)^2. \quad (12)$$

There are five parameters in the drop rate functions chosen for the parameter fitting. Due to limited experimental data, especially with systems with different physical properties, all of the parameters could not be identified properly. Thus, C_3 was set to 0.2 and C_5 to 2000 at the last phase of the fitting procedure, and three parameters, namely C_1 , C_2 , and C_4 were left to be optimized. The frozen coefficient values were obtained by reasoning from the extrapolation studies with different physical properties, and these should not be considered to have any other but order of magnitude accuracy. It must also be noted that the parameters and functional forms are not independent, but a consistent set of equations and corresponding parameters must be used whenever drop size distributions are calculated.

Results from the Single Block Model

In the single block model, three parameters were fitted along with the two estimated. Three measured steady state population distributions were used, one before the step change to higher impeller speed, one after the change, and one after the step change back to the lower value. Besides that, two transient distributions after the step change to higher impeller speed were used. In all these distributions, the Sauter mean diameter and the population densities at four locations of the distribution were used. Hence, totally 25 experimental points were used in the fitting procedure.

The optimal fitted parameter values for the single block model were $C_1 = 0.986$, $C_2 = 0.892 \cdot 10^{-3}$, and $C_4 = 0.433 \cdot 10^{-3}$. The estimated Sauter mean diameters were quite close to the average measured values, as can be seen from the Figure 3. Some deviation remains in the population density distribution, as shown in Figure 4.

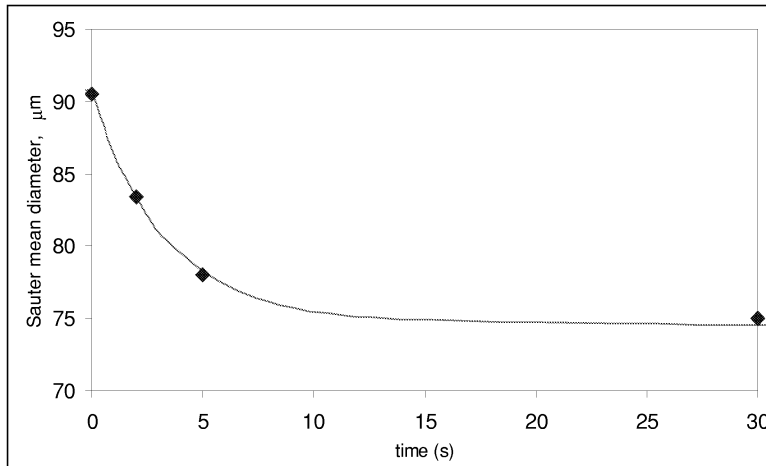


Figure 3. Simulated and measured Sauter mean diameters for averaged vessel properties during transient between two steady states.

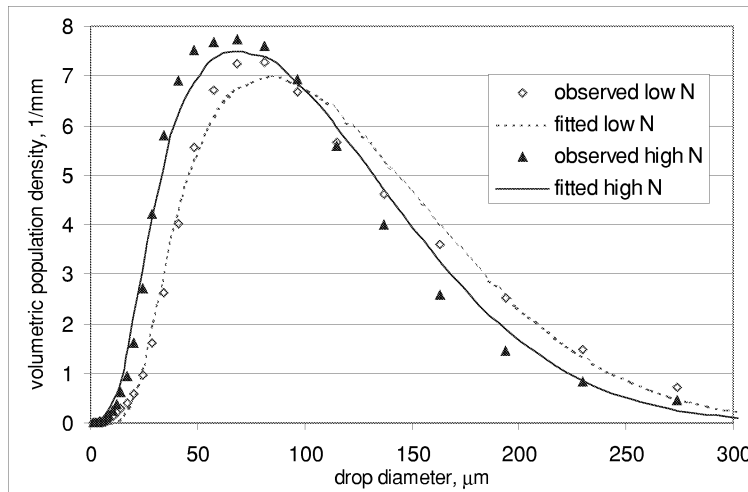


Figure 4. Simulated and measured volumetric population densities for averaged vessel properties at steady states.

Results from the Multiblock Model

In the multiblock model, we have two sources of transient data for the population balance parameter fitting. The first one is to use the transient data as the impeller speed is altered, similarly to the single block model. The other source is vessel inhomogeneity from both the steady state measurements, and measurements taken during the transients. As the dispersion flows into the impeller region, the drops are broken, and during the circulation, they collide and coalesce. Then the parameters for the breakage functions can be fitted separately by measuring the drop size distributions at different points in the circulation region. The longer the time period over which the distributions are measured (time-averaged), the more accurate are the results. Thus, parameter fitting with the multiblock model and different measuring points should give more reliable parameter values than the single block model with only transients in impeller speed. Another source of error, when the transient response data is used, is that the flow fields are assumed to reach their new steady states immediately after the step change in impeller speed. For turbulent energy dissipation, this may be a reasonable assumption, but for flow fields, there are transients of a few seconds even for small-scale vessels. A problem with the measurements at different locations in the vessel is that the measuring probe may slightly alter the flow fields. Of course, if the measured drop size distribution is entirely homogeneous, then the transient parameters cannot be identified by using local measurements.

The drop rate functions were the same than in the single block model. The optimized parameter values for the multiblock model were $C_1 = 3.68$, $C_2 = 0.775 \cdot 10^{-3}$, and $C_4 = 1.55 \cdot 10^{-3}$. In Figure 5, measured and fitted Sauter mean diameters from two blocks are shown. These correspond to the measurement points 1 and 3 of Figure 2.

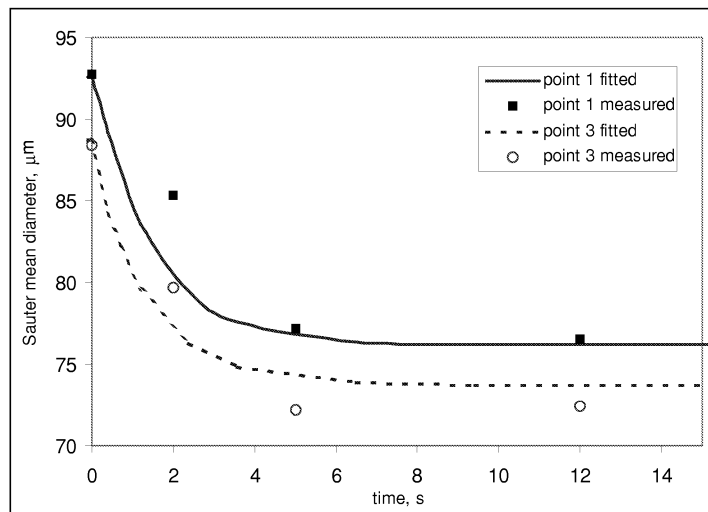


Figure 5. Simulated and measured Sauter mean diameters in the multiblock model during transient.

The inhomogeneity in the vessel was from 4 to 6 % in the Sauter mean diameter. The calculated population distributions are shown in Figure 6. Even though the inhomogeneity was quite small due to a small scale stirred tank, it was enough to be used as a source of data in the parameter fitting.

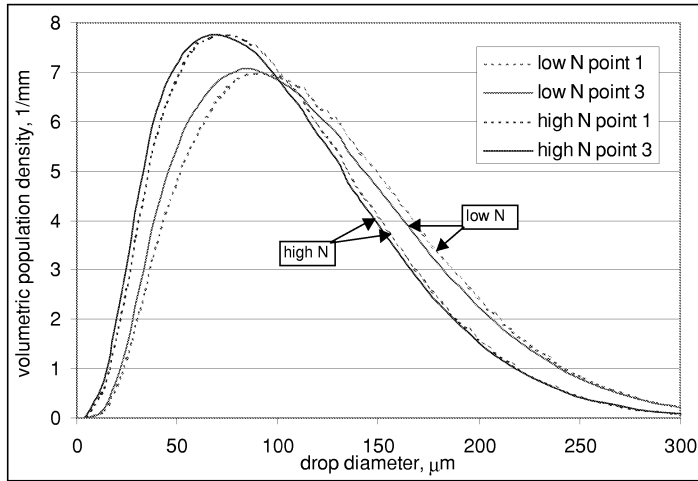


Figure 6. Simulated population densities at two locations of the vessel with two impeller speeds.

Conclusion

The drop rate function parameters were fitted with experimental data measured on-line from a dense liquid-liquid dispersion in a stirred tank. The fitting procedure was carried out for both averaged vessel turbulence properties, and with the multiblock model where detailed turbulence conditions and flow fields are used. A reasonably good fit was obtained in both cases. It seems that the available measurement technique is the most uncertain part of this approach, but as the techniques are developing, the present approach becomes a more practical design tool.

The fitting procedure revealed that the multiblock model is a useful tool when used along with the population balances. Measuring and fitting the parameters with the local drop size distribution proved to be an applicable approach describing the dispersion in the vessel more

accurately than the averaged vessel modeling. The present model is flexible for any degree of complexity of the fluid flow, and therefore can be used in a great variety of situations including liquid-liquid dispersions. In addition, CFD can be used in a rather easy and straightforward manner to model flow and turbulence values needed in the multiblock model. In most industrial cases reliable measurements are not available and new measurements are too expensive.

Acknowledgments

Financial support from Neste Oy Foundation and the Brite Euram program, contract number BRPR-CT96-0185, are gratefully acknowledged. Finally, we would like to thank the Laboratory of Chemical Engineering, Lappeenranta University of Technology, Lappeenranta, Finland, for carrying out the measurements.

Notation

$\#(V_i)$	index number of drop class of characteristic volume V_i
Δa	width of droplet class (m)
a	drop diameter (m)
a_{32}	Sauter mean diameter, $a_{32} = \Sigma a_i^3 / \Sigma a_i^2$, (m)
$C_1 \dots C_5$	empirical constants
D_i	impeller diameter (m)
$F(a_i, a_j)$	binary coalescence rate between droplets a_i and a_j in unit volume ($\text{m}^3 \text{s}^{-1}$)
$g(a)$	breakage frequency of drop size a (s^{-1})
$h(a_i, a_j)$	collision frequency between droplets a_i and a_j in unit volume ($\text{m}^3 \text{s}^{-1}$)
N	impeller speed (s^{-1})
N_P	impeller power number
N_Q	impeller pumping number
Q	flow rate ($\text{m}^3 \text{s}^{-1}$)
$Q^*_{i,j}$	dimensionless flow rate from subregion i to j
r	radial coordinate (m)
t	time (s)
V	Total tank volume (m^3)
V_i	Volume of a subregion i (m^3)
Y_i	number concentration of drop class i (m^{-3})
$Y_{i,\text{in}}, Y_{i,\text{out}}$	flow of drop class i per unit volume into and out from the region of interest, respectively ($\text{s}^{-1} \text{m}^{-3}$)
z	axial coordinate (m)

Greek symbols

$\beta(a_i, a_j)$	probability that a drop of size a_i is formed when a_j breaks (m^{-1})
ε	average turbulent energy dissipation (per unit mass) (m^2 / s^3)
$\varepsilon(z,r)$	local turbulent energy dissipation (m^2 / s^3)
$\lambda(a_i, a_j)$	collision efficiency between droplets a_i and a_j
μ_D, μ_C	dispersed phase and continuous phase viscosities (Pa s)
$\nu(a)$	number of drops formed when drop of size a is broken
ρ_D, ρ_C	dispersed phase and continuous phase densities (kg / m^3)
σ	interfacial tension (N/m)
φ	relative turbulent energy dissipation
ϕ	volume fraction of dispersed phase

Literature Cited

Alopaeus, V., Koskinen, J., Keskinen, K. I., Simulation of the Population Balances for Liquid-Liquid Systems in a Nonideal Stirred Tank, Part 1 Description and Qualitative Validation of the Model, *Chem. Eng. Sci.* **54** (1999) pp. 5887-5899.

Bapat, P. M., Tavlarides, L. L., Smith, G. W., Monte Carlo Simulation of Mass Transfer in Liquid-Liquid Dispersions, *Chem. Eng. Sci.* **38** (1983) pp. 2003-2013.

Bourne, J. R., Yu, S., Investigation of Micromixing in Stirred Tank Reactors Using Parallel Reactions, *Ind. Eng. Chem. Res.* **33** (1994) pp. 41-55.

Coulaloglou, C. A., Tavlarides, L. L., Description of Interaction Processes in Agitated Liquid-Liquid Dispersions, *Chem. Eng. Sci.* **32** (1977) pp. 1289-1297.

Haley, I., Lasentec, Private communication (1999).

Narsimhan, G., Gupta, J. P., Ramkrishna, D., A Model for Transitional Breakage Probability of Droplets in Agitated Lean Liquid-Liquid Dispersions, *Chem. Eng. Sci.*, **34** (1979) pp. 257-265.

Tadayyon, A., Rohani, S., Determination of Particle Size Distribution by Par-Tec® 100: Modeling and Experimental Results, *Part. Part. Syst. Charact.* **15** (1998) pp. 127-135.